THE ASTROPHYSICAL JOURNAL, 166:593–603, 1971 June 15

ABUNDANCES IN OPEN CLUSTERS: MODEL-ATMOSPHERE ABUNDANCE ANALYSIS OF STARS IN THE PLEIADES AND HYADES CLUSTERS

FREDERIC H. CHAFFEE, JR.
Smithsonian Astrophysical Observatory, Cambridge, Massachusetts

DUANE F. CARBON
Smithsonian Astrophysical Observatory and Department of Astronomy, Harvard University, Cambridge, Massachusetts

AND

STEPHEN E. STROM
State University of New York at Stony Brook, Long Island, and Smithsonian Astrophysical Observatory

Received 1970 July 2; revised 1971 February 2

ABSTRACT

Detailed analysis of six F and G dwarfs in the Pleiades and fourteen in the Hyades indicates that the Fe/H ratio in the Hyades is 50 percent higher than that in the Pleiades, the latter yielding the solar value.

To gain insight into the cause of the differences in observed narrow-band photometric indices between the clusters, a grid of blanketed model atmospheres was computed. The models provide estimates of the changes in the Strömgren four-color indices caused by variations in the metal abundance z and the microturbulent velocity ξ. The trajectories in the $(m_1, b - y)$-plane resulting from either of these variations are similar and difficult to distinguish observationally. The trajectories in the $(c_1, b - y)$-plane, however, differ significantly, and in some cases this may permit these two atmospheric parameters to be distinguished by the photometry alone.

In the case of the Pleiades and Hyades, it appears that the observed differences in ξ and z can explain the photometric differences between the clusters. However, the effects of initial helium content and stellar evolution considerably complicate the interpretation of the Strömgren diagrams of these clusters; interpretation is even more difficult for more heterogeneous samples of stars.

I. INTRODUCTION

In many recent studies of stellar-abundance and evolution problems, the Hyades Cluster has been adopted as a standard against which all other clusters are compared. However, its photometric properties appear to be somewhat anomalous compared with other galactic clusters. For example, the Strömgren m_1 and c_1 indices for the stars in the Hyades differ significantly from those in the Pleiades (Crawford 1969), Coma, and Ursa Major (Crawford and Barnes 1969) clusters. Increased blanketing resulting from systematically higher metal abundances in the Hyades (Wallerstein and Helfer 1959) has been proposed as a possible cause for the higher observed values for the m_1 indices (Parker *et al.* 1961; Helfer and Wallerstein 1964). An alternative explanation has been offered by Conti and Deutsch (1966, 1967). They argue that m_1 is sensitive to the microturbulence parameter and suggest the possibility that blanketing effects resulting from microturbulence and abundance differences can be confused. However, no explanation has been offered for the anomalous behavior of the c_1 index. Because there appears to be no correlation between c_1 and m_1 excess and/or deficiency, c_1 is thought to be unaffected by metal content or turbulence. In this investigation, we propose first to analyze a selection of Hyades and Pleiades dwarfs in order to determine accurately the abundance and microturbulence values appropriate to these clusters. Second, we will attempt to predict from blanketed model atmospheres the behavior of the photometric indices and to obtain accurate values for z and ξ.

II. OBSERVATIONAL DATA

Six F and G dwarfs in the Pleiades and fourteen in the Hyades were selected for analysis. Spectra were obtained by R. P. Kraft in the region between 3800 and 4800 Å with dispersions of 9 and 10 Å mm^{-1}. At this dispersion the problem of blending is acute. To circumvent this difficulty, we carefully selected the unblended lines in Table 1 from an examination of the revised Rowland atlas (Moore, Minnaert, and Houtgast 1966). The spectra were reduced to intensity against wavelength tracings by use of the digitized David Mann microphotometer at the Harvard College Observatory. The computer program MICRO (Latham 1967) was of considerable help in expediting this phase of the analysis. Equivalent widths of the selected Fe I lines were determined by planimetering intensity tracings, and these are given in milliangstroms for each star in Table 1. The Hyades spectra were exposed to a sufficiently high density redward of $H\beta$ to allow us to measure additional Fe I lines. Throughout this paper, the van Bueren (1952) numbers are used to identify the Hyades dwarfs, and the Hertzsprung II (1947) numbers to identify those in the Pleiades.

III. ABUNDANCE AND MICROTURBULENCE DETERMINATIONS

The next step in the analysis is the selection of an appropriate atmospheric model for each star. This requires knowledge of the effective temperature $T_{\rm eff}$, the surface gravity g, and the heavy-metal content z relative to the solar value.

The derived abundances of iron by use of Fe I lines are quite sensitive to $T_{\rm eff}$ in this spectral range [log (Fe/H) changes by 0.10 for every change of 250° K in $T_{\rm eff}$], and care must be taken in selecting a consistent set of effective temperatures for all stars.

Values of $T_{\rm eff}$ were obtained by combining the Johnson (1966) calibration of the (spectral type, $T_{\rm eff}$)-relation with the (spectral type, $b - y$)-relation for the field stars (Crawford 1969). A slightly different ($T_{\rm eff}$, $b - y$)-relation results when the Hyades (spectral type, $b - y$)-relation is used. In the spectral region we are considering, however, the value of $T_{\rm eff}$ inferred from $b - y$ is insensitive ($< \pm 40°$ K) to whether the Hyades or field-star (spectral type, $b - y$)-relation is used.

We are grateful to Dr. Crawford for providing the four-color and $H\beta$ photometry for the Pleiades in advance of publication. Interpretation of the Pleiades cluster photometry is somewhat complicated by variable interstellar reddening across the face of the cluster. However, since the β index is unaffected by reddening, it can be used to predict the intrinsic $b - y$ of each star and thus its $T_{\rm eff}$ value. The c_1 and m_1 indices can also be corrected for reddening by using the relations given by Crawford (1966).

Originally the surface gravities were obtained from Eggen's (1963) mass-luminosity relations for the Hyades and Sun-Sirius groups (the latter being applied to the Pleiades) by use of the known location of the program stars in the (L, $T_{\rm eff}$)-plane. Distance moduli of 5.70 and 3.04 were adopted for the Pleiades (Anderson, Stoeckly, and Kraft 1966) and Hyades (Wayman, Symms, and Blackwell 1965), respectively. It should be noted that Eggen's (1963) suggestion that the Hyades have a high helium content would increase the mean molecular weight in the atmospheres of the Hyades. At $T_{\rm eff}$ values appropriate to F dwarfs, this change results in an increase in the stellar surface gravity. However, the value of Fe/H obtained from Fe I lines in this spectral range is insensitive to the choice of log g (the deduced abundance does not change in the range $4.0 \leq \log g \leq 4.3$); thus, we have adopted a value of $\log g = 4.3$ as appropriate for all the dwarfs.

Finally, as a starting value for the analysis, a metal/hydrogen ratio of $z = 1$ (the solar values of Goldberg, Müller, and Aller 1960) was adopted. The resulting abundances are insensitive to this assumption provided that z does not vary by more than a factor of 3.

The characteristics of the models and the method used for the abundance determinations have been described by Conti and Strom (1968). We have used the Corliss and

TABLE 1

EQUIVALENT WIDTHS OF Fe I LINES

	Hyades														Pleiades					
λ	10	15	17	18	29	39	50	52	58	63	97	102	119	122	405	739	948	1726	1766	1797
4325.76	586	760	792	760	628	864	710	695	837	678	—	654	560	562	455	520	644	390	261	402
4365.90	48	35	—	61	—	53	50	52	72	49	—	43	—	49	70	41	76	45	46	26
4375.93	224	232	220	283	155	274	238	254	278	201	—	237	169	210	165	183	175	150	76	115
4383.55	730	1002	830	1030	718	1035	908	900	1031	954	900	855	704	750	567	—	624	463	307	388
4404.75	650	827	843	780	544	893	710	697	896	792	711	680	553	515	440	512	584	416	312	316
4415.12	435	610	628	610	480	686	595	568	639	578	575	535	479	455	421	441	617	315	349	289
4443.20	155	234	211	241	193	211	242	201	231	184	230	215	187	184	160	155	153	146	79	83
4447.72	187	221	—	232	167	200	198	167	250	182	193	197	167	153	142	190	199	135	119	101
4485.68	100	120	85	97	83	104	113	102	115	113	108	96	104	85	74	90	128	63	88	56
4547.85	81	95	82	98	47	73	97	89	110	79	81	72	85	86	71	59	104	76	74	38
4602.00	74	102	85	87	48	77	72	70	70	61	56	63	46	51	33	—	69	49	26	23
4602.94	175	191	162	152	112	172	159	139	188	120	148	153	130	131	112	—	135	95	85	80
4661.98	50	65	72	—	—	—	—	68	64	64	73	95	64	—	29	—	37	—	25	—
4700.17	73	64	63	90	69	75	54	60	95	65	53	73	49	89	46	—	139	50	—	29
4788.76	73	106	89	69	—	87	94	56	89	64	54	74	73	—						
4835.86	77	53	58	125	67	108	134	97	127	119	—	—	—	72						
4872.14	300	273	306	312	183	312	287	271	296	294	244	228	225	187						
4890.76	266	321	219	324	246	371	262	298	369	351	273	256	287	200						
4891.50	330	300	383	370	262	415	285	319	406	384	297	307	294	222						
4892.87	76	81	—	71	—	—	—	60	72	44	44	66	46	—						
4917.24	58	55	74	78	—	65	52	—	45	79	69	72	48	36						
4919.00	305	313	364	314	234	420	266	292	367	354	300	296	267	240						
4920.51	384	377	418	425	294	506	378	384	475	456	374	348	350	317						
4946.40	130	106	101	150	82	105	91	—	121	125	119	—	92	111						

TABLE 2

ABUNDANCE PARAMETERS FOR CLUSTER STARS

Star	Sp	$(b-y)_0$	m_1	c_1	T_{eff} (° K)	−log Fe/H	ξ (km sec^{-1})
				Hyades			
10.....	G0	0.374	0.209	0.325	5840	5.28±0.08	3.5
15.....	G3 V	...	...	...	5700	5.21±0.08	2.7
17.....	G5 V	...	...	...	5660	5.28±0.10	3.4
18.....	G2	...	...	...	5770	5.17±0.11	4.1
29.....	F8 V	0.352	0.194	0.371	6000	5.17±0.12	2.5
39.....	G5	...	...	...	5660	5.16±0.12	3.2
50.....	G1 V	0.386	0.200	0.325	5750	5.24±0.11	3.5
52.....	G1 V	0.384	0.204	0.327	5760	5.28±0.11	3.2
58.....	G6 V	...	...	...	5550	5.32±0.09	4.0
63.....	G5 V	...	...	...	5660	5.36±0.12	3.6
97.....	G1 V	...	...	...	5825	5.21±0.11	3.0
102.....	G1 V	0.384	0.214	0.331	5760	5.35±0.10	3.5
119.....	F8	0.356	0.195	0.353	5970	5.23±0.10	3.0
122.....	F5	0.351	0.180	0.364	6000	5.24±0.09	3.0
Mean:						5.25±0.06	3.3
				Pleiades			
405.....	F7 V	0.343	0.181	0.371	6060	5.43±0.11	2.0
739.....	G1 V	0.392	0.193	0.298	5720	5.47±0.12	1.75
948.....	F8 V	0.377	0.196	0.367	5830	5.32±0.12	2.5
1726.....	F7 V	0.304	0.182	0.382	6220	5.37±0.06	2.0
1766.....	F5 V	0.253	0.177	0.448	6670	5.29±0.10	1.75
1797.....	G0 V	0.347	0.182	0.322	6030	5.64±0.08	0.25
Mean:						5.42±0.13	1.7

Warner (1964) transition probabilities for all lines, and in all cases damping constants of 10× classical were adopted.

Table 2 contains the relevant atmospheric parameters for the program stars and the deduced values of log (Fe/H) and ξ. We estimate the accuracy of ξ to be ±0.5 km sec^{-1}, and the errors quoted for log (Fe/H) are the probable errors.

The Hyades dwarfs yield an average value of log (Fe/H) that is higher than that for the Pleiades dwarfs by 0.17. In addition, the mean value of ξ in the Hyades is higher than that in the Pleiades.

We have also reanalyzed three Hyades giants, using the equivalent widths from Helfer and Wallerstein (1964). The model parameters and the resulting abundances for Fe I (85 lines) and Fe II (25 lines) are given in Table 3. The effective temperatures for γ, δ, and ϵ Tau have been inferred from the wide-band infrared photometry of

TABLE 3

ABUNDANCE PARAMETERS FOR HYADES GIANTS

Star	T_{eff} (° K)	log g	$-\log (Fe/H)_{Fe\,I}$	$-\log (Fe/H)_{Fe\,II}$	ξ (km sec^{-1})
γ Tau.....	5000	2.5	5.46±0.03	5.56±0.03	4.0
δ Tau.....	5000	2.5	5.50±0.03	5.65±0.03	4.0
ϵ Tau.....	5000	2.5	5.27±0.03	5.56±0.04	4.0

Johnson *et al.* (1966) and from Johnson's (1966) temperature calibration. Since the scatter in the Fe II abundance determinations is somewhat smaller than that for Fe I, the Fe II lines were used to obtain the values of ξ. However, the iron abundance deduced from the Fe II lines is quite sensitive to log g (0.4 dex when log g is varied from 1.5 to 2.5), whereas that deduced from the Fe I lines changes by only 0.02 when log g is varied between 1.5 and 3.0. Therefore, the abundance deduced from the Fe I lines should be used for comparison between the dwarfs and the giants. We feel that the discrepancies between the iron abundances deduced from the neutrals and the ions are insignificant since the abundances can be brought into coincidence by a very small adjustment in the value of log g. The difference of 0.15 in log abundance between the giants and dwarfs is not easily interpreted. However, a different set of lines and consequently a different set of f-values and equivalent widths could produce a discrepancy of this magnitude.

Finally, to provide a basis for comparison, we have computed the solar iron abundance from the 14 Fe I lines that were used in the analysis for both the Pleiades and the Hyades dwarfs. Equivalent widths for these lines were taken from the Rowland atlas, and the Bilderberg continuum atmosphere (Gingerich and de Jager 1968) was used for the analysis. The solar iron abundance obtained in this way is -5.40 ± 0.10 with $\xi = 1.5$ km sec^{-1}. The f-value scale of Corliss and Warner was used in this determination; since we are interpreting all results in a differential sense, the absolute accuracy of this scale does not affect the subsequent discussion.

IV. PHOTOMETRIC DIFFERENCES AND LINE BLANKETING

a) Blanketed Models

Photometric studies of the Hyades have shown that the dwarfs have weaker (more heavily blanketed) ultraviolet continua than most other stellar aggregates that have been studied in any detail. This observed behavior could be ascribed to a higher abundance of metals in the atmospheres of its members. A higher metal content on first glance would also appear to be consistent with the somewhat higher values of m_1 observed for the Hyades. However, the effects of microturbulence must be considered since the Hyades appear to have high ξ as well.

Figures 1 and 2 are the unreddened (m_1, $b - y$)- and (c_1, $b - y$)-diagrams for the

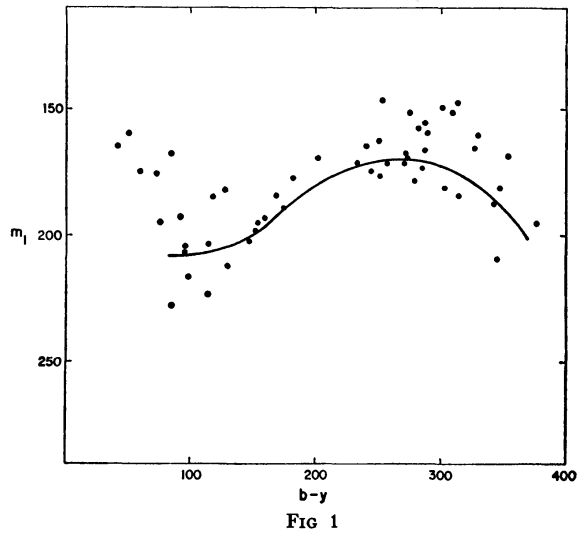

FIG 1

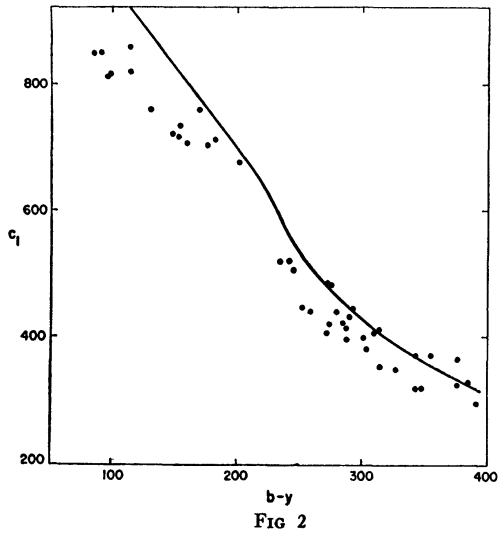

FIG 2

FIG. 1.—Pleiades (m_1, $b - y$)-diagram (*solid curve*, Hyades mean relation).

FIG. 2.—Pleiades (c_1, $b - y$)-diagram (*solid curve*, Hyades mean relation)

Pleiades. The solid curves are the Hyades standard relations taken from Crawford and Perry (1966). The figures clearly show the systematically high m_1 and c_1 indices in the Hyades.

Conti and Deutsch (1966, 1967) have described the dependence of the m_1 index on metal abundance and microturbulence in solar-type stars. Their analysis, however, is based solely on estimates of line blocking from high-dispersion spectra and does not take into account the differences in the atmospheric temperature structure caused by the increased line opacity. Moreover, no prediction of the c_1 index behavior was made by these authors. In order to determine the dependence of the emergent flux upon metal abundance and ξ, one of us (D. F. C.) has constructed line-blanketed model atmospheres for stars with $T_{\rm eff} = 6000°$ and 6500° K.

Since the basic method for constructing the blanketed model atmospheres has been discussed in detail by Carbon and Gingerich (1969), we shall review it only briefly here. The metal-line blanketing is represented in the models by a frequency- and depth-dependent triple picket. One step of the picket is chosen to represent the average opacity characteristic of line cores; another, to represent the average wing opacity. The third step contains only the continuous opacity. A large number of representative lines were calculated in models constructed at effective temperatures of 6500°, 5781°, and 4000° K. From an examination of the results, representative curves for the depth dependence of the metal-line opacity were determined. The frequency weights of the picket opacities for each of six spectral regions were calculated by means of a simple algorithm that relates the weights to the observed blocking coefficients, $\eta(\lambda_1, \lambda_2)$:

$$\eta(\lambda_1, \lambda_2) \equiv \int_{\lambda_1}^{\lambda_2} (F_\lambda^c - F_\lambda) d\lambda \Big/ \int_{\lambda_1}^{\lambda_2} F_\lambda^c d\lambda \,,$$

where F_λ^c is the continuous flux at wavelength λ, interpolated if necessary, and F_λ is the actual flux. Once the frequency weights and depth dependences for the picket levels have been established, only the strengths of the blanketing opacities remain to be specified. These were treated as free parameters and were varied until agreement was obtained between the observed and the calculated values of $\eta(\lambda_1, \lambda_2)$ in each spectral region. This process was repeated for each of the models with normal z and ξ employed here. These normal dwarf models are essentially identical with those presented by Carbon and Gingerich except that we have ignored convection in this investigation.

b) The Lower Main Sequence

The models with variations in z were calculated at 6000° and 6500° K. For the 6000° K model, the strengths of the picket opacities were multiplied by factors of 1.25, 1.5, and 2.0 to mimic the effect of 1.25×, 1.5×, and 2.0× changes in metal abundance, respectively. For the 6500° K model, only a 2× model was computed. In all cases, the abundances of all the metals were multiplied by the appropriate amount in the solution of the equation of state. The models were driven to a flux constancy of better than 1 percent throughout.

Additional variation models were calculated at the same effective temperatures in order to determine the effects of changes in microturbulent velocity. For these models, it was assumed that the microturbulent velocity had changed from 2.0 to 2.5 km sec^{-1}. This corresponds to an increase of approximately 15 percent in the Doppler parameter for Fe lines in the temperature range considered here. In order to approximate the behavior of the metal-line opacities, the widths of the picket levels (core and wing) were increased by 15 percent and the strengths of the opacity steps decreased by 15 percent. Once again, the models were driven to better than 1 percent flux constancy.

By combining the predicted emergent fluxes and the transmission functions of the

Strömgren four-color filters, we have calculated the changes in each of the four-color indices caused by changes in ξ and z. No attempt has been made to predict the absolute values of the colors; only the *changes* at a given temperature are computed. These results are summarized in Table 4 for the indicated changes in z and ξ. Photometric changes are given in thousandths of a magnitude, and the results are presented graphically in Figures 3 and 4. The vectors labeled Δz are the trajectories that a 1× blanketed star would follow if its metal abundance were increased by a factor of 1.50 (0.18 in log z). The solid and dashed curves are the Hyades and Pleiades mean relations, respectively. The vectors labeled $\Delta\xi$ are similar trajectories for stars whose microturbulent velocities have been increased by 25 percent. As a basis for comparison, the blocking trajectories of Conti and Deutsch for the Sun for the same z and ξ changes have been included in Figure 3. Since our calculations take into account the differences in the temperature structure caused by the increased blanketing whereas those of Conti and Deutsch do not, it is not surprising that our trajectories differ somewhat from theirs.

The mean $b - y$ for the six Pleiades dwarfs ($\langle b - y\rangle = 0.336$) is considerably lower than that for the fourteen Hyades dwarfs. Since the Strömgren system is seldom used beyond $b - y = 0.400$, only half the Hyades dwarfs in Table 1 have measured $b - y$ values. We can estimate, however, that the mean $b - y$ for the Hyades dwarfs is greater than 0.400. Chaffee (1970) has suggested that in the spectral range of middle F to early G, the microturbulent velocity in field stars increases. In light of this, we suspect that the higher values of ξ in Table 1 for the Hyades dwarfs compared with the Pleiades dwarfs are simply a reflection of the later mean spectral types of the former compared with the latter. Therefore, although we have calculated changes in the Strömgren diagrams resulting from changes in both ξ and z, we feel that $\Delta z = 1.5$ and $\Delta\xi = 0$ should be adopted as the simplest assumption (to be revised if necessary) when comparing the Hyades and Pleiades diagrams.

Because the Δz and $\Delta\xi$ trajectories are nearly parallel on the lower main sequence in

TABLE 4

PREDICTED PHOTOMETRIC CHANGES CAUSED BY ABUNDANCE AND MICROTURBULENCE ENHANCEMENT

	$b-y$		
PARAMETER	0.350	0.278	0.132
$T_{\rm eff}$ (° K)	6000	6500*	7500
$z_2/z_1=1.25$:			
$\Delta(b-y)$	+ 7	+ 7	+13
Δm_1	+10	+ 3	− 4
Δc_1	+24	+13	+15
$z_2/z_1=1.50$:			
$\Delta(b-y)$	+15	+15	+14
Δm_1	+22	+ 7	+11
Δc_1	+25	+14	+19
$z_2/z_1=2.0$:			
$\Delta(b-y)$	+17	+17	+21
Δm_1	+56	+16	+31
Δc_1	+47	+26	+21
$\xi_2/\xi_1=1.25$:			
$\Delta(b-y)$	+ 6	+ 1	...
Δm_1	+15	+12	...
Δc_1	− 7	+ 1	...

* Only the 2× model was calculated explicitly. The 1.25× and 1.50× values were scaled from 2.0× by use of the corresponding entries from the 6000° K model.

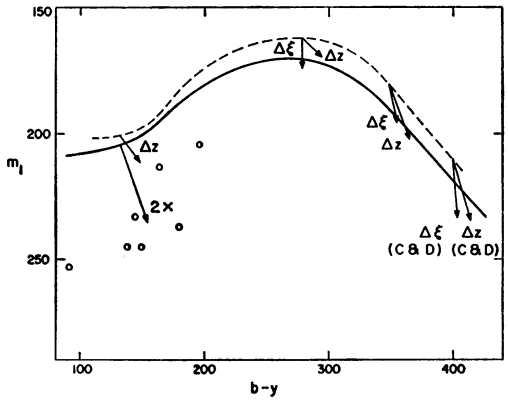

FIG 3

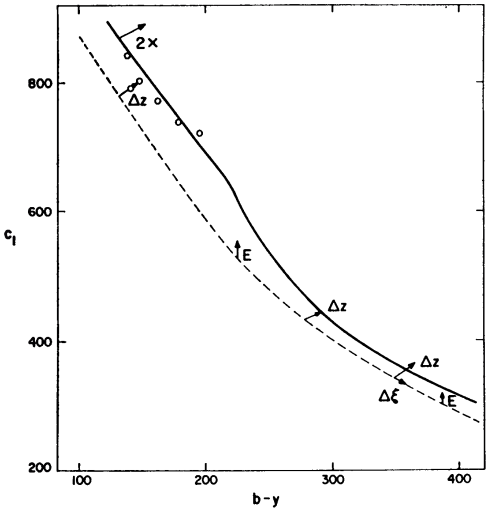

FIG 4

FIG. 3.—Photometric changes in the (m_1, $b - y$)-diagram caused by a metal-abundance increase of 50 percent (Δz) and a microturbulence increase of 25 percent ($\Delta\xi$) between the Pleiades (*dashed line*) and Hyades (*solid line*) clusters. Vectors labeled (C & D) are the trajectories of Conti and Deutsch (1966, 1967). Vector labeled 2× represents a 2× increase in metal abundance. *Open circles*, Hyades Am stars.

FIG. 4.—Photometric changes in the (c_1, $b - y$)-diagram caused by a metal-abundance increase of 50 percent (Δz), a microturbulence increase of 25 percent ($\Delta\xi$), and evolutionary changes (E) between the Pleiades (*dashed line*) and Hyades (*solid line*) clusters. Vector labeled 2× represents a 2× increase in metal abundance. *Open circles*, Hyades Am stars.

Figure 3, it is clear that from the (m_1, $b - y$)-diagram alone, blanketing caused by increased metals or increased microturbulence cannot be distinguished. An increase in z by a factor of about 1.3 results in the same m_1 changes as an increase of 25 percent in ξ. However, in Figure 4 the $\Delta\xi$ and Δz trajectories for the lower main sequence are nearly perpendicular to each other, and the photometric effects caused by changes in z and ξ should be separable.

We should add a note of caution for those wishing to apply our trajectories to observed Strömgren indices. First, as shown in Table 4, the changes in the indices caused by changes of 1.25×, 1.5×, and 2.0× are not simple and monotonic. Interpolation in this table should thus be carried out carefully. Second, calculations show that the effect of a simultaneous change in ξ *and* z will not be the simple sum of their individual vectors, since these effects are not uncoupled. Finally, the behavior of the flux through any filter is dependent on several parameters (primarily the *detailed* distribution in frequency and strength of the lines in the filter passband) that can only be approximated by the present technique. More accurate blanketing trajectories can be calculated when a more detailed representation for the blanketing opacity becomes available for the model atmospheres (e.g., Strom and Kurucz 1966). In view of these cautionary remarks, we suggest that Table 4 be used only to explain trends and not the exact locations of stars in observed Strömgren diagrams.

c) The Upper Main Sequence

Although we have not carried out abundance analyses for stars on the upper main sequence, understanding the behavior of the photometry in this region is nonetheless important to an overall understanding of the differences between the Pleiades and the Hyades. We have selected $T_{\rm eff}$ = 7500° K as representative of stars in this region. At

this temperature, the microturbulent velocity differs considerably from the solar value (e.g., Conti and Strom 1968; Chaffee 1970; Smith 1971), and we have adopted $\xi = 7.0$ km sec^{-1} as representative of these stars. For observed blocking coefficients, we employed the values estimated for the Hyades A stars by Dr. M. Breger, to whom we are grateful for providing these data in advance of publication. Using these blocking coefficients and the techniques described earlier, blanketed models at $T_{\rm eff} = 7500°$ K were constructed with different metallicities. Changes in the Strömgren indices for Δz of 1.25×, 1.5×, and 2.0× are given in Table 4, and the vector changes resulting from $\Delta z = 1.5\times$ are plotted in Figures 3 and 4.

The models at 7500° K are very sensitive to the choice of the η's and of ξ, and no simple linear interpolation applies to the resulting vector changes. In particular, the m_1 changes are very sensitive in the range $1.25\times \leq \Delta z \leq 1.5\times$. In light of the uncertainties in both the models and the abundance analyses, we feel that the differences in the upper main sequence in the Strömgren diagrams for the clusters can be explained by a metal enhancement in the Hyades that is entirely consistent with the value derived from our high-dispersion analysis of the later-type dwarfs. We should mention, however, that we would be unable to explain the photometric differences between the Hyades and the Pleiades clusters if we were to use the very high metal abundances in the Hyades found by Nissen (1970).

It is of further interest to attempt to explain the location of the Hyades Am stars. We adopt $z = 2\times$ as typical of these stars, and the changes in the Strömgren diagrams are shown in Figures 3 and 4. The open circles are the Hyades Am stars, and the vector changes begin on the Hyades mean relation since we wish to explain the location of these stars relative to the normal Hyades dwarfs. The positions of the Am stars in the (m_1, $b - y$)-diagram are readily explained by a 2× increase in their metal abundances over the normal stars. The vector change in the (c_1, $b - y$)-diagram, however, would seem to suggest that the Am stars in the cluster should lie above the main sequence, whereas, as the open circles indicate, they lie either on or slightly below it. This apparent discrepancy may be explained by considering the relative rotational velocities of the Am and normal A stars. As a result of their rotation, the normal Hyades A stars, whose mean $v \sin i$ is 100 km sec^{-1} (Kraft 1965), will be displaced from the zero-rotation main sequence because of a decreased effective temperature (increased $b - y$) and a decreased surface gravity (increased c_1). Unfortunately, no quantitative estimate of the displacement of these indices as a function of rotation is available. Nevertheless, the *direction*, if not the magnitude, of the rotation effect is clear. The Am stars are displaced from the zero-rotation main sequence in the same direction because of their increased metal abundance. Thus both sets of A stars lie on nearly the same *observed* main sequence, even though the physical parameters that determine their locations differ.

d) Evolutionary Effects

Because of the age difference between the clusters, we must consider the effects of evolution on the four-color indices before attributing the observed behavior of the indices to either ξ or z. Using Iben's (1967) evolutionary tracks, we have estimated the effect of this age difference on the c_1 and m_1 indices. We have used Table III and Figure 2 of Iben's paper to estimate the changes in L and $T_{\rm eff}$ for the Hyades stars (assuming an age of 10^9 years) and the Pleiades stars (assuming an age of 2×10^8 years). We can then compute the differences $\Delta T_{\rm eff}$ and $\Delta \log L$ between the Hyades and Pleiades main sequences; these can be converted to corresponding changes in the photometric indices $\Delta(b - y)$ and Δc_1.

The evolutionary change in c_1 has two components: the first is due to the change in luminosity ($\Delta M_{\rm bol}$), and the second to the change in effective temperature. The $\Delta M_v/\Delta c_1$ ratios compiled by Crawford (1966) were used to determine the first component, while the second was obtained using the mean Pleiades (c_1, $b - y$)-relation.

Since the Paschen continuum is relatively insensitive to surface gravity in this temperature range, there is no luminosity component to the evolutionary change in m_1. The change in m_1 due to $\Delta(T_{\rm eff})$ was obtained by use of the mean Pleiades (m_1, $b - y$)-diagram. The small evolutionary changes we are considering simply slide stars along the main sequence in the (m_1, $b - y$)-diagram. Hence, only the (c_1, $b - y$)-diagram will be affected by the early evolutionary changes, and the vectors labeled "E" in Figure 4 show these changes for stars having 1.0 and 1.25 solar masses.

The possible uncertainty in the relative initial helium content of the clusters further complicates the interpretation of the (c_1, $b - y$)-diagram since the ages derived for the clusters as well as the details of the evolution beyond the turnoff point depend critically on the choice of Y, the helium abundance. Bodenheimer (1965) has determined the location of the zero-age main sequence (ZAMS) for normal ($Y = 0.34$) and helium-rich ($Y = 0.62$) stars. The latter choice was based on Eggen's (1963) estimate of the helium abundance of the Hyades. From Bodenheimer's calculations, we estimate that at a given effective temperature, the value of log g for a star on the helium-rich ZAMS and that for a star on the normal ZAMS can differ by as much as 0.15. This would imply that the helium-rich ZAMS would lie 0.035 below the normal ZAMS in c_1. This uncertainty makes it difficult for us to attribute the four-color differences between two clusters to any single physical phenomenon such as metal abundance or microturbulence anomalies. Provided, however, that the initial helium abundance of the Pleiades and that of the Hyades are the same, their Strömgren diagrams appear to be satisfactorily explained by the high value of z in the Hyades.

In light of these results, we feel that four-color photometry can be used to infer variations in z or ξ only *within* a given cluster or between clusters where the initial helium content of the stars is the same. Finally, it is quite clear that extreme caution must be exercised in interpreting the four-color photometry (or any similar intermediate-band photometric system) of any heterogeneous sample of stars.

V. SUMMARY

We have established the following points:

1. Model-atmosphere abundance analyses of Fe I lines in the Hyades and Pleiades dwarfs reveal that the Hyades have higher Fe/H values by about 50 percent.

2. The changes in the four-color photometric indices caused by microturbulence and abundance variations have been calculated by use of the predicted emergent fluxes from line-blanketed model atmospheres. These results suggest that microturbulence and metal-abundance effects can be distinguished photometrically. Evolutionary effects complicate the interpretation of the photometry. However, if the Pleiades and Hyades have the same initial helium abundance, their Strömgren diagrams are satisfactorily explained by the derived 50 percent metal enhancement in the Hyades.

These calculations further indicate that the Strömgren c_1 index is *not* independent of blanketing. Therefore, Δc_1 should be used with caution as a luminosity indicator among a sample of stars whose abundances and/or microturbulences are significantly abnormal.

The authors wish to thank Dr. David L. Crawford for many illuminating discussions concerning the photometry.

REFERENCES

Anderson, C. M., Stoeckly, R., and Kraft, R. P. 1966, *Ap. J.*, **143**, 299.
Bodenheimer, P. 1965, *Ap. J.*, **142**, 451.
Bueren, H. G. van. 1952, *B.A.N.*, **11**, 385.
Carbon, D. F., and Gingerich, O. 1969, in *Theory and Observation of Normal Stellar Atmospheres*, Proc. Third Harvard-Smithsonian Conference on Stellar Atmospheres, ed. O. Gingerich (Cambridge, Mass.: MIT Press), p. 377.

Chaffee, F. H. 1970, *Astr. and Ap.*, **4**, 291.
Conti, P. S., and Deutsch, A. J. 1966, *Ap. J.*, **145**, 742.
———. 1967, *Ap. J.*, **147**, 368.
Conti, P. S., and Strom, S. E. 1968, *Ap. J.*, **152**, 483.
Corliss, C. H., and Warner, B. 1964, *Ap. J. Suppl.*, **8**, 395.
Crawford, D. L. 1966, in *Spectral Classification and Multicolour Photometry*, Proc. I.A.U. Symposium No. 24, ed. K. Loden, L. O. Loden, and U. Sinnerstad (New York: Academic Press), p. 170.
———. 1969, private communication.
Crawford, D. L., and Barnes, J. V. 1969, *A.J.*, **74**, 407.
Crawford, D. L., and Perry, C. L. 1966, *A J.*, **71**, 206.
Eggen, O. J. 1963, *Ap. J. Suppl.*, **8**, 125.
Gingerich, O., and Jager, C. de. 1968, *Solar Phys.*, **3**, 5.
Goldberg, L., Müller, E. A., and Aller, L. H. 1960, *Ap. J. Suppl.*, **5**, 1.
Helfer, H. L., and Wallerstein, G. 1964, *Ap. J. Suppl.*, **9**, 81.
Hertzsprung, E. 1947, *Leiden Ann.*, **19**, part 1.
Iben, I., Jr. 1967, *Ann. Rev. Astr. and Ap.*, **5**, 571.
Johnson, H. L. 1966, *Ann. Rev. Astr. and Ap.*, **4**, 193.
Johnson, H. L., Mitchell, R. I., Iriarte, B., and Wisniewski, W. Z. 1966, *Comm. Lunar and Planet. Lab.*, **4**, 99.
Kraft, R. P. 1965, *Ap. J.*, **142**, 681.
Latham, D. W. 1967, *Smithsonian Ap. Obs.*, private distribution.
Moore, C. E., Minnaert, M. G. J., and Houtgast, J. 1966, *N.B.S. Monog.*, No. 61 (Washington, D.C.: Government Printing Office).
Nissen, P. E. 1970, *Astr. and Ap.*, **6**, 138.
Parker, R., Greenstein, J. L., Helfer, H. L., and Wallerstein, G. 1961, *Ap. J.*, **133**, 101.
Smith, M. S. 1971, Ph.D. dissertation, in preparation.
Strom, S. E., and Kurucz, R. L. 1966, *J. Quant. Spectrosc. and Rad. Transf.*, **6**, 591.
Wallerstein, G., and Helfer, H. L. 1959, *Ap. J.*, **129**, 347.
Wayman, P. A., Symms, L. S. T., and Blackwell, K. C. 1965, *R.O.B.*, No. 98.